Experimental characterization of the diffuse incident angle modifier of solar thermal collectors: improving consistency between test methods

J. M. Rodríguez-Muñoz[a,*], I. Bove[b], R. Alonso-Suárez[a,b]

[a] *Laboratorio de Energía Solar, Departamento de Física del Litoral, CENUR Litoral Norte, Universidad de la República*
[b] *Laboratorio de Energía Solar, Instituto de Física, Facultad de Ingeniería, Universidad de la República*

Abstract

Diffuse solar irradiance is essential for modeling solar energy conversion devices, especially solar thermal collectors. The globally accepted ISO 9806:2017 standard defines a thermodynamic model and two test methods to determine its parameters, the steady-state test (SST) and the quasi-dynamic test (QDT). Although both methods are generally considered equivalent, discrepancies between the values of the diffuse incident angle modifier (IAM) have been reported, representing an area for improvement. This study advances the experimental characterization of diffuse IAM, specifically improving the compatibility between SST and QDT methods. Using the ISO 9806:2017 model as a baseline, two alternative diffuse IAM models are introduced and experimentally evaluated with data from a flat plate collector and an evacuated tube collector, covering different technologies. Model 1 extends the SST diffuse IAM model to QDT and treats diffuse irradiance in a global manner, while Model 2 treats diffuse irradiance from sky and ground separately, requiring an additional solar measurement. The evaluation shows that both proposed models improve the consistency between test methods. As the performance differences between these two new models are minimal, Model 1 is the recommended option as its implementation is simpler.

Keywords: Solar thermal collector, diffuse incident angle modifier, ground albedo, ISO 9806 standard.

1. Introduction

Diffuse solar irradiance is important for modeling solar devices such as solar thermal collectors. In mid-latitude temperate climates, around 1/3 of the annual global horizontal irradiation is diffuse [1]. The widely accepted international ISO 9806:2017 standard [2] offers a thermodynamic model to estimate useful power from solar thermal collectors and includes two testing methods to determine its parameters: Steady State Testing (SST) and Quasi-Dynamic Testing (QDT). Although other standards exist, such as ASHRAE-93 [3], they are highly similar, essentially making them equivalent to each other [4].

*Corresp. author: J. M. Rodríguez-Muñoz, jrodrigue@fing.edu.uy

List of Symbols

$\dot{Q}_u$	Useful power produced by the collector, W.
$\eta_{0,b}$	collector peak efficiency referred to direct solar irradiance.
$\eta_{0,hem}$	collector peak efficiency referred to global solar irradiance.
θ	Incidence angle.
θ_L	Longitudinal angle of incidence.
θ_T	Transversal angle of incidence.
ϑ_a	Ambient air temperature, °C.
ϑ_i	Collector inlet temperature, °C.
ϑ_m	Mean temperature of heat transfer fluid, °C.
ϑ_o	Collector outlet temperature, °C..
a_1	Heat loss coefficient, $\mathrm{W/m^2K}$.
a_2	Temperature dependence of the heat loss coefficient, $\mathrm{W/m^2K^2}$.
a_5	Effective thermal capacity, $\mathrm{J/Km^2}$.
A_G	Gross area of collector, $\mathrm{m^2}$.
f_d	Diffuse fraction, G_{dt}/G_t.
G_{bt}	Direct solar irradiance on collector plane, $\mathrm{Wm^{-2}}$.
G_b	Direct normal solar irradiance, $\mathrm{Wm^{-2}}$.
G_{dg}	Diffuse solar irradiance on the collector plane reflected by the ground, $\mathrm{Wm^{-2}}$.
G_{dh}	Diffuse solar irradiance on horizontal plane, $\mathrm{Wm^{-2}}$.
G_{ds}	Diffuse solar irradiance on collector plane from the sky, $\mathrm{Wm^{-2}}$.
G_{dt}	Diffuse solar irradiance on collector plane, $\mathrm{Wm^{-2}}$.
G_h	Global solar irradiance on horizontal plane, $\mathrm{Wm^{-2}}$.
G_t	Global solar irradiance on collector plane, $\mathrm{Wm^{-2}}$.
K_b	Incidence angle modifier for direct solar irradiance.
K_d	incidence angle modifier for diffuse solar irradiance.
K_{bL}	Incidence angle modifier in the longitudinal plane.
K_{bT}	Incidence angle modifier in the transversal plane.
K_{dg}	incidence angle modifier for diffuse solar irradiance reflected by the ground.
K_{ds}	incidence angle modifier for diffuse solar irradiance from the sky.
K_{hem}	Incidence angle modifier for global solar irradiance.
q	Volumetric flow rate, $\mathrm{L\,min^{-1}}$.
u	Surrounding air speed, $\mathrm{m\,s^{-1}}$.

The Incidence Angle Modifier (IAM) is an important part of the above-mentioned thermodynamic model that takes into account the variation of the optical efficiency with the angle of incidence and the environmental conditions. This modeling is addressed with two parameters, one for each component of the solar irradiance, direct and diffuse, namely K_b and K_d, respectively. The importance of direct-diffuse modeling disaggregation in energy performance calculations has been demonstrated in Ref. [5]. In our previous work, an improved direct IAM model (K_b) was proposed, originally developed for flat plate collectors [6] and then extended to evacuated tube collectors [7]. This model shows better performance than the other available models and is suitable for general use; it can be applied to collectors with uniaxial or biaxial IAM. This study builds on these previous efforts and focuses specifically on the other part of IAM modeling: the improvement of the diffuse IAM (K_d). As in the previous work, the ISO 9806:2017 standard model is used as a baseline.

In both test methods of ISO 9806:2017 (SST and QDT), diffuse solar irradiance is modeled globally by a single parameter, K_d, which remains constant for a given collector. Although this is the most usual approach, it should be noted that it does not distinguish, for example, the different contributions to the diffuse irradiance from the sky by atmospheric scattering and from the surroundings by reflection, nor their different directionality. The two test methods differ in the way this global diffuse parameter is estimated. In the SST method, K_d is derived indirectly from K_b, the latter being determined experimentally through a specific sub-test. Specifically, to estimate K_d in the SST framework, the previously determined K_b function is integrated and weighted over the solid angle seen by the collector, assuming an isotropic distribution of diffuse solar irradiance. In the QDT method, the parameter K_d is determined directly from experimental data, addressing some anisotropic effects in the solar irradiance distribution. This creates a clear contrast in the treatment of K_d between the two test methods, which has led to discrepancies between them [7–10], i.e. the values of K_d obtained by one method and the other show differences. In the case of flat plate collectors, the differences are small, on the order of 5 %, so the useful power estimated by both methods is similar [11]. In contrast, for evacuated tube collectors, the differences are significant and increase with diffusion fraction and temperature differences, reaching 39 % in the worst case [7].

To reduce these differences, Rodríguez-Muñoz et al. [7] propose an improved parameter conversion procedure from SST to QDT that incorporates the diffuse solar irradiance measurements into the standard procedure. This procedure has been implemented for two different ETC-HP collectors, and the advantages over the standard procedure have been demonstrated. It reduces the differences between SST and QDT in the parameters related to the optical efficiency, in particular the K_d parameter. However, the reduction in differences is partial and further research is needed to improve the consistency between test methods. This motivates the present work, which focuses on improving the modeling and consistency of the K_d parameter within the ISO 9806:2017 framework. Although alternative approaches exist, for various reasons, these approaches have not been incorporated into the testing standards, as will be discussed in the following paragraphs.

One of the alternative approaches to modeling K_d in the QDT method is derived from the work of Bosanac et al. [12]. In this work, experiments with a flat plate collector were performed using in-situ measurements. Although the procedure and model used are not exactly those of the standard, the methodology is similar to that of the QDT method. Specifically, this author proposes modeling K_d based on K_b, similar to the SST method; K_b is integrated and weighted over the solid angle seen by the collector, globally, without distinguishing between that from the sky and that reflected from the ground. The implementation of this model in the standard QDT method may allow greater consistency with the SST method. However, this has not yet been tested. Another research gap is that other types of collectors, such as evacuated tubes, have not yet been tested. Finally, the main disadvantage is that the parameter identification process is more complex and requires a non-linear regression algorithm.

Another alternative is proposed by Carvalho et al. [13], who suggest modifying the SST method by calculating K_d separately, using two different parameters instead of one. One parameter accounts for diffuse radiation from the sky, while the other accounts for ground-reflected radiation. This author introduces a calculation procedure for these new parameters, similar to the SST method, but with customized integration limits for each case. This model has been experimentally evaluated for both a flat plate collector and an evacuated tube collector, demonstrating the advantages of this approach [5]. However, the model has not been implemented in the QDT method. It is important to mention that Carvalho et al.'s model was originally proposed by Brandemuehl and Beckman [14] and later adopted in various textbooks in the field of solar energy [15]. This author has contributed to the integration of the model into the standard and has gone further to demonstrate its applicability to different solar collector technologies and orientations.

Finally, the work of Hess and Hanby [16] is highlighted. Continuing the work of Carvalho et al., it incorporates an anisotropic distribution in the calculation procedure of the parameter associated with the diffuse solar irradiance from the sky [17], introducing precision as well as computational complexity. This work illustrates the advantages of this model over previous models at moderate operating temperatures for a flat plate collector with reflectors through numerical analysis. However, at low operating temperatures and/or traditional flat collectors, no advantages appear. In line with these results, in Ref. [18] the diffuse solar transmittance of a common flat glazing was analyzed and the anisotropic model of Hess and Hanby was adapted and compared with the traditional isotropic assumption. Both models were evaluated with experimental data for two different glass orientations. The results show that the anisotropic model is superior to the isotropic model, but the differences are very small and do not compensate for the additional computational complexity of the anisotropic model. For this reason, in the context of the present work, the anisotropy of the diffuse solar irradiance from the sky is considered as a second-order effect.

1.1. Article's contribution

The main objective of this work is to advance in the experimental characterization of the diffuse IAM (K_d), improving the compatibility between thermal performance test methods. In this sense, two alternative models (Model 1 and Model 2) are proposed to address this problem.

These models are based on the models of Bosanac et al. and Carvalho et al. and seek to fill the research gap of these previous works. Specifically, the integration of these models into the ISO 9806:2017 framework is detailed for both SST and QDT test methods, and their applicability is experimentally demonstrated using test data from two solar collectors: a flat plate collector (FPC) and an evacuated tube collector with heat pipes (ETC-HP). These collectors have very different IAM characteristics so that the results can be easily extrapolated to a wide range of collectors. The advantages and disadvantages of each approach are identified, and guidelines for improving the test standard are proposed.

The first model (Model 1) extends the K_d modeling of the SST methodology to QDT. Although this

model was originally proposed by Bosanac et al. for FPC, in this work we show its applicability to the standard QDT method and demonstrate its applicability to ETC technology. In the second model (Model 2), we propose a separate modeling of the diffuse irradiance, distinguishing between that coming from the sky and that reflected from the ground, as proposed by Carvalho et al. for the SST method. In this case, unlike the previous study [13], the specific implementation for the QDT method is presented and compared with SST. This model is more accurate in predicting the useful power of the collector. However, it has the disadvantage of requiring an additional measurement of the solar irradiance, i.e. the diffuse solar irradiance reflected by the ground. In this sense, a simple method for estimating this component is proposed, which requires the prior characterization of the albedo of the ground surrounding the test bed. Nevertheless, it is also shown that substantial variations in the albedo estimation do not significantly affect the test results, which is experimentally demonstrated in this work, evidencing the robustness of this method.

With respect to the experimental evaluation of the models, it is shown that both approaches provide more robust results compared to the standard model by improving the consistency between the test methods. It is also shown that although Model 2 outperforms Model 1, the differences are small, making it difficult to compensate for the additional cost of implementing an additional solar irradiance measure. Therefore, we consider that Model 1 is the best option for improving the test standard. In addition, it is also shown that this model can be used to characterize a specific collector, and then Model 2 can be used to estimate its energy production in a long-term simulation, for a specific site and usage conditions, taking full advantage of each model.

Furthermore, the improved parameter conversion from SST to QDT proposed in Ref. [7] has been extended and evaluated in combination with the diffuse IAM models considered in this work. This approach further improves the consistency between the test methods, especially in the case of the ETC-HP collector.

An important drawback of both models is that the parameter identification procedure in the case of the QDT method requires a non-linear regression algorithm, which adds complexity and makes it difficult to replicate. In this context, a free and documented Matlab program is provided to perform the parameter identification, facilitating the reproduction of the QDT method and the integration of the alternative diffuse IAM models into the test standard.

By addressing the above, the following scientific and technical contributions are provided in this work:

- The diffuse IAM models proposed by Bosanac et al. and Carvalho et al. are implemented within the current ISO 9806 framework for both the SST and QDT test methods for the first time, and guidelines are provides for its posterior use in long-term performance simulations.

- The applicability of these models is demonstrated experimentally for two solar collector technologies, FPC and ETC, reducing discrepancies between steady-state and quasi-dynamic test methods, a well recognized problem in the field of solar thermal collector testing.

- A simple and robust method is proposed to measured diffuse solar irradiance reflected from the ground in the framework of QDT method, minimizing the need for additional solar irradiance instruments.
- The improved parameter conversion procedure proposed by Rodríguez-Muñoz et al. [7] is extended, showing that its use, in combination with these diffuse IAM models, further reduces test method discrepancies.
- A free and well-documented MATLAB program is provided for parameter identification, facilitating the reproduction of the QDT method and the integration of the aforementioned models.

1.2. Article's outline

The structure of this work is presented as follows. In the next section, Section 2, the thermodynamic model proposed by the ISO standard is presented for the collector technologies considered in this work, along with the experimental procedure for each test method. This section also shows the integration of the alternative diffuse IAM models into the standard test methods: SST and QDT. Section 3 describes the test platform and the experimental data used in this work, in particular the procedure for obtaining the diffuse solar irradiance reflected by the ground, which is required for the implementation of Model 2. Additionally, this section outlines the methodology used to assess the performance comparison of the alternative diffuse IAM models with respect to the standard model. Section 4 presents the results obtained, and finally, Section 5 summarizes the main conclusions of this work.

2. Thermodynamic model and testing methods

This section describes the thermodynamic model used in the test standard, the procedure for each test method, and provides a detailed description of the alternative diffuse IAM model and its integration into the standard.

2.1. Standard thermodynamic model

The thermodynamic model defined in the ISO 9806:2017 standard is general enough to be applied to different solar collector technologies. The standard also provides guidelines for adapting the model to specific cases, specifying which terms can be omitted from the general equation based on the solar collector technology used. Eq. (1) presents the recommended model for low temperature glazed collectors,

$$\frac{\dot{Q}_u}{A_G} = \eta_{0,b}\left[K_b\left(\theta\right)\ G_{bt} + K_d\ G_{dt}\right] - a_1\left(\vartheta_m - \vartheta_a\right) - a_2\left(\vartheta_m - \vartheta_a\right)^2 - a_5\frac{d\vartheta_m}{dt}, \tag{1}$$

where $\dot{Q}_u$ is the useful power produced by the collector; G_{bt} and G_{dt} are the direct and diffuse solar irradiances on the collector plane, respectively; ϑ_m is the mean temperature of the fluid flowing through the collector (mean between the inlet and outlet temperatures); ϑ_a is the ambient temperature; and the

parameters characterizing the thermal behavior of the collector are $\eta_{0,b}$, K_b, K_d, a_1, a_2 and a_5. The first parameter is the optical efficiency of the collector at normal incidence with respect to direct solar irradiance, a_1 and a_2 are the thermal loss factors, and a_5 is the effective thermal capacity divided by the total collector area (A_G). As introduced earlier, K_b and K_d characterize the IAM with respect to direct and diffuse solar irradiance, respectively.

All parameters remain constant except K_b, which varies as a function of the angle of incidence of the direct beam, θ. In this work, for this function we have used the model proposed in Ref. [6, 7] due to its wide applicability (uniaxial or biaxial IAM) and its superior performance compared to other models available in the scientific literature. This model consists of dividing the incident angle range into smaller intervals and assuming a piecewise linear function within each interval. For example, if a 10° interval is used, the adjustable parameters would be $K_b(10°), K_b(20°), \ldots, K_b(80°)$, where $K_b(\theta_i)$ represents the K_b value at angle θ_i. For all types of collectors, it is mandatory that $K_b(0°) = 1$ and $K_b(90°) = 0$ for the first and last parameters, respectively. In the case of ETC, the standard factorization approach was used [2], i.e. the IAM was expressed as the product of two different functions: one dependent on θ_L and the other dependent on θ_T, denoted as $K_b = K_{bL} \times K_{bT}$. Here K_{bL} is K_b calculated at $(\theta_L, 0)$ and K_{bT} is K_b calculated at $(0, \theta_T)$. The discretization process described above was applied to both the K_{bL} and K_{bT} functions.

The QDT method uses the model directly presented in Eq. (1). The SST method, however, uses a simpler model that treats solar radiation globally. This involves the following substitution,

$$\eta_{0,b}\left[K_b\left(\theta\right)\ G_{bt} + K_d\ G_{dt}\right] = \eta_{0,hem} K_{hem} G_t, \tag{2}$$

leading to the following model,

$$\frac{\dot{Q}_u}{A_G} = \eta_{0,hem} K_{hem} G_t - a_1\left(\vartheta_m - \vartheta_a\right) - a_2\left(\vartheta_m - \vartheta_a\right)^2 - a_5 \frac{d\vartheta_m}{dt}. \tag{3}$$

Here G_t is the global irradiance at the collector plane. The parameters $\eta_{0,hem}$ and K_{hem} correspond to the optical efficiency at normal incidence and the incident angle modifier, both with respect to the global solar irradiance. It is noteworthy that in the SST model, the parameter C is commonly used to characterize the effective thermal capacity of the collector. However, in order to reduce the number of parameters and maintain homogeneity, a_5 was chosen as an alternative. The relationship between C and a_5 is expressed as $a_5 = C/A_G$.

The procedure for estimating QDT parameters from SST parameters (parameter conversions), i.e., estimating $\eta_{0,b}$, K_b, and K_d from $\eta_{0,hem}$ and K_{hem}, is detailed in Annex B of ISO 9806:2017. This procedure is described as follows. First, to estimate K_d, clear sky conditions are assumed, so $K_{hem} = K_b$. Then, K_b is averaged and normalized over the solid angle seen by the collector, assuming an isotropic distribution for

diffuse solar irradiance. That is,

$$K_d = \frac{\int_0^{\pi/2}\int_0^{\pi/2} K_b\left(\theta,\gamma\right)\cos\left(\theta\right)\sin\left(\theta\right)d\theta d\gamma}{\int_0^{\pi/2}\int_0^{\pi/2}\cos\left(\theta\right)\sin\left(\theta\right)d\theta d\gamma}. \tag{4}$$

The standard recommends performing this integral as a summation by discretising the integration domain into intervals of length 10°, an approach used in this study. The parameter $\eta_{0,b}$ is then calculated from Eq. (2) assuming normal incidence and a diffuse fraction of 15 % in the plane of the collector, which is reasonable for SST conditions. That is,

$$\eta_{0,b} = \frac{\eta_{0,hem}}{0.85 + 0.15 \times K_d}. \tag{5}$$

2.2. Test procedure

This section describes the data collection procedure for each test method. It should be noted that in each case the test variables must meet certain stability requirements, as specified in the respective test standard and summarized in various works, such as Ref. [4]. This work can be consulted if the reader is interested in a deeper study of these requirements.

2.2.1. Quasi dynamic testing method

In the QDT method, parameter identification is performed by a single test, which requires the execution of at least one measurement sequence for each day type. Each day type corresponds to a specific measurement sequence as defined in the standard. The total number of sequences required depends on the local climatic conditions and the timing of the test. Each day type must be at least 3 hours in duration and may consist of several non-consecutive sub-sequences of at least 30 minutes each. There are four different day types, and the conditions that must be met for each are detailed in the following paragraph.

Day type 1 focuses on running sequences where the fluid temperature is close to the ambient temperature, emphasizing clear sky conditions. The angle of incidence varies within a specified range, providing sufficient variability for K_b function. Day type 2 involves measurements under varying cloud conditions at any operating temperature. Day type 3 requires the collector to operate at an intermediate inlet temperature, with measurements including clear sky conditions at two different intermediate temperatures. Day type 4 requires a high inlet temperature sequence, including clear sky measurements.

To ensure that the experimental data set contains sufficient variability for accurate parameter identification, the standard recommends that the following plots be generated: 1) $(\vartheta_m - \vartheta_a)$ as a function of G; 2) G_{bt} as a function of θ; 3) G_{dt} as a function of G; and 4) $(\vartheta_m - \vartheta_a)$ as a function of u. These plots must be compared to the typical plots of the standard and should show a significant degree of similarity.

2.2.2. Steady state testing method

In the SST method, parameter determination involves three distinct tests: (i) a performance test to determine the parameters $\eta_{0,hem}$, a_1, and a_2; (ii) an incident angle modifier test to determine K_{hem}; and (iii) an effective thermal capacity test to determine the parameter a_5. The first test is extensively documented and discussed in several references [4], so a detailed description is omitted here.

For the second test (IAM determination), we followed the same procedure as for day type 1 of the QDT test, but the experimental data were processed according to the SST methodology. For each angle of incidence, the experimental IAM value was determined using Eq. (3). The final IAM value for a given angle of incidence was calculated as the average between two measurements: one before and one after solar noon (symmetrical), taking into account transient effects (a fixed tracker was used for this test).

Both the current and previous tests; performance and IAM, must be conducted under steady-state conditions, ensuring that $d\vartheta_m/dt \approx 0$. Once these tests are complete, the parameter conversion procedure described in the previous section must be performed.

The effective thermal capacity test was conducted following section 25.2 of the ISO 9806:2017 standard, considering the second-order adjustment in thermal losses, i.e., the a_2 coefficient. At the beginning of the test, the inlet temperature was set equal to the ambient temperature, and the collector was covered with a reflective blanket to reach a steady state. Subsequently, the cover was removed, and the collector was allowed to reach a new steady-state point, which differed from the initial one due to the effect of solar irradiance. The effective thermal capacity was determined by integrating Eq. (3) over the time period between the two stationary operating points.

2.3. Diffuse incident angle modifier

In this study, two alternative models for K_d are considered, referred to as Model 1 and Model 2, in addition to the standard model (Model 0) which serves as the baseline. For Model 0, the parameter K_d is computed using Eq. (4) within the SST method, following the procedure outlined above. In the QDT method, however, this parameter is derived directly from the experimental data.

In Model 1, the procedure for estimating K_d in the SST method remains unchanged, and this model is extended to QDT. In other words, Eq. (4) is incorporated into Eq. (2), so that K_d is no longer fitted directly from the data. Instead, it depends directly on the nodal values of K_b, which are determined along with the rest of the parameters in the parameter identification algorithm. This change improves the overall consistency between the test methods because both models treat K_d in the same manner and, for a given collector, the parameter K_d corresponds to a constant value.

Model 2 differs from the previous models in the way it treats diffuse solar irradiance. While both Model 0 and Model 1 treat diffuse solar irradiance globally, Model 2 makes a distinction between diffuse solar irradiance coming from the sky and that reflected from the ground, with a parameter for each component:

K_{ds} and K_{dg}, respectively. The calculations for these parameters are given below,

$$K_{ds} = \frac{\int_0^{\pi/2}\int_0^{\zeta} K_b(\theta,\gamma)\cos(\theta)\sin(\theta)d\theta d\gamma + \int_{\pi/2}^{\pi}\int_0^{\pi/2} K_b(\theta,\gamma)\cos(\theta)\sin(\theta)d\theta d\gamma}{\int_0^{\pi/2}\int_0^{\zeta}\cos(\theta)\sin(\theta)d\theta d\gamma + \int_{\pi/2}^{\pi}\int_0^{\pi/2}\cos(\theta)\sin(\theta)d\theta d\gamma}, \tag{6}$$

$$K_{dg} = \frac{\int_0^{\pi/2}\int_{\zeta}^{\pi/2} K_b(\theta,\gamma)\cos(\theta)\sin(\theta)d\theta d\gamma}{\int_0^{\pi/2}\int_{\zeta}^{\pi/2}\cos(\theta)\sin(\theta)d\theta d\gamma}. \tag{7}$$

Here, β corresponds to the horizontal tilt of the collector, and $\zeta = \arctan\left[(-\tan\beta\cos\gamma)^{-1}\right]$. In this case, for a given collector, the parameters K_{ds} and K_{dg} vary as a function of the horizontal tilt of the collector. These expressions assume symmetry with respect to the longitudinal plane of the collectors.

Two observations are made about these equations. The first observation is that in the original paper by Carvalho et al., these integrals were expressed in a different coordinate system. In this paper, the choice has been made to use the same coordinate system as ISO 9806:2017, θ and γ, thus maintaining greater homogeneity and consistency with the standard, and facilitating model integration. The second observation is that in the case of collectors with biaxial K_b, for example, evacuated tube collectors, the function K_b is written in terms of the angles θ_L and θ_T, as already mentioned. Therefore, to perform the integrals, these angles must be expressed in terms of θ and γ. These relations are provided in the ISO 9806:2017 standard.

Finally, below is an explanation of how Model 2 is incorporated into the thermodynamic model of the standard and into the SST and QDT test methods. In the case of the thermodynamic model, Eqs. (6) and (7) are incorporated directly into the model of Eq. (1) by the following substitution,

$$K_d\ G_{dt} = K_{ds}\ G_{ds} + K_{dg}\ G_{dg}, \tag{8}$$

leading to the following model,

$$\frac{\dot{Q}_u}{A_G} = \eta_{0,b}\left[K_b(\theta)\ G_{bt} + K_{ds}\ G_{ds} + K_{dg}\ G_{dg}\right] - a_1(\vartheta_m - \vartheta_a) - a_2(\vartheta_m - \vartheta_a)^2 - a_5\frac{d\vartheta_m}{dt}, \tag{9}$$

where G_{ds} and G_{dg} are the diffuse solar irradiance at the collector plane, coming from the sky and reflected from the ground, respectively.

In both test methods, the integration of this model takes place at the data processing level. In the case of the SST method, the parameter conversion procedure changes and now requires the estimation of the parameters $\eta_{0,b}$, K_b, K_{ds} and K_{dg} (new thermodynamic model) from $\eta_{0,hem}$ and K_{hem}. The procedure is described as follows. First, to estimate K_d, clear sky conditions are assumed, so $K_{hem} = K_b$, as before. Then the parameters K_{ds} and K_{dg} are calculated using Eqs. (6) and (7). Finally, the parameter $\eta_{0,b}$ is estimated as follows,

$$\eta_{0,b} = \frac{\eta_{0,hem}}{0.85 + 0.12 \times K_{ds} + 0.03 \times K_{dg}}. \tag{10}$$

This equation results from combining Eq. (5) and Eq. (8). In addition, it was assumed that 15 % accounts for diffuse solar irradiance, distributed as 12 % from the sky and 3 % reflected from the ground, a reasonable hypothesis for clear sky conditions and low reflective ground.

2.4. Parameter identification algorithm for QDT

Regarding the parameter identification algorithm for the QDT method, there are two options [11], which differ in how they treat transient phenomena. The first method involves approximating the time derivative using finite differences and treating it as an independent variable in a regression algorithm commonly known as multi-linear regression (MLR). Its name derives from its use in the context of flat-plate collector testing [19]. The second method is to perform a dynamic simulation coupled with a non-linear regression algorithm (Dynamic Parameter Identification, DPI). Although its implementation is more challenging, it offers significant advantages as it better handles the transient effects of solar collectors, both under standard test conditions and in situ conditions as demonstrated in Refs. [20, 21]. As a result, it provides more reliable parameter estimations. . This method is particularly suitable for ETC-HP technology, as experimentally demonstrated in Ref. [18], technology addressed in the present work.

In this work, the DPI procedure was used, as it provides more reliable results and therefore offers a better framework for comparing diffuse IAM models. Given the difficulty of its implementation, a Matlab program for parameter identification is provided here, which represents a continuation and improvement of the code provided in Ref. [18]. This program facilitates the implementation and reproduction of the QDT methodology and the integration of the alternative diffuse IAM models in the test standard.

The program also reports uncertainty values for performance parameters (i.e., all parameters except those related to the beam IAM) using the linearization approach, which is simple and provides reliable results [20]. However, this method can only estimate uncertainty for parameters that represent input variables within the regression algorithm. Since the parameters of the proposed diffuse IAM models are not adjustable themselves but are instead calculated from the beam IAM, it is not possible to assign uncertainty to them. Other uncertainty estimation methods exist for the DPI approach, such as bootstrapping and Monte Carlo methods [22, 23], which allow estimation of the uncertainty of these parameters. However, these methods are more complex, computationally intensive, and do not provide additional insights for the specific objective of diffuse IAM modeling, and were therefore not considered in this work. Nevertheless, this remains a topic for future work.

3. Experimental data and methodology

This section provides a description of the test facilities, in particular, the diffuse solar irradiance measurements that are central to this work. It also describes the collectors considered, the experimental data, and the methodology used to assess the performance of the alternative diffuse IAM models.

3.1. Test facilities

The experiments were carried out at the Solar Heater Test Bench (Banco de Ensayos de Calentadores Solares - BECS) located at the Solar Energy Laboratory (Laboratorio de Energía Solar - LES, http://les.

edu.uy/) of the University of the Republic in the city of Salto, Uruguay (latitude=31.28° S, longitude=57.92° W). This test bench, originally designed by LES researchers, is based on existing facilities of the Spanish National Renewable Energy Center (Centro Nacional de Energías Renovables - CENER). Notably, this test facility recently participated in a Latin American laboratory intercomparison organized by the PTB (Physikalisch-Technische Bundesanstalt), Germany's national metrology institute. It received the highest ratings in most of the test variables and only had two minor observations regarding the determination of secondary variables, both of which were already addressed by the laboratory [24].

The thermo-hydraulic installation and the data acquisition system are described in detail in Ref. [6], so they will not be reproduced here. However, we provide a description of the instrumentation dedicated to solar irradiance measurements, with particular emphasis on diffuse solar irradiance, a crucial aspect of this study.

In this regard, the facility is equipped with three Kipp & Zonen CMP10 pyranometers. These pyranometers measure global solar irradiance in the collector plane (G_t), as global and diffuse solar irradiance in the horizontal plane (G_h and G_{dh}, respectively). All pyranometers used are spectrally flat and classified as class A according to the ISO 9060:2018 standard [25]. They are calibrated annually at LES with the ISO 9847:2023 standard [26] against a Kipp & Zonen CMP22 secondary standard traceable to the World Radiometric Reference at the World Radiation Center in Davos, Switzerland. The diffuse irradiance measurement is mounted with a shadow band, so the raw measurements must be corrected. For this correction, the expression given in Ref. [27] has been used, which is significantly better than the correction suggested by the manufacturer [28].

Parameter identification in the SST method requires the measurement of global solar irradiance at the collector plane for the diffuse IAM models analyzed. However, the QDT method requires separate estimation of its direct and diffuse components. Therefore, the following information is provided on how each component was estimated at the collector plane.

The direct solar irradiance G_{bt} at the collector plane was estimated from G_h and G_{dh} using the following procedure. First, the direct normal irradiance (DNI, G_b) was calculated using the closure relation $G_h = G_b \cos\theta_z + G_{dh}$, where $\cos\theta_z$ is the cosine of the solar zenith angle. Then G_{bt} was calculated from the DNI by multiplying it by the cosine of the angle of incidence, θ. The diffuse solar irradiance G_{dt} at the collector plane was estimated from G_t and G_{bt}, simply by the difference, i.e. $G_{dt} = G_t - G_{bt}$. This diffuse measurement includes both the diffuse irradiance from the sky and the diffuse irradiance reflected from the ground (G_{ds} and G_{dg}, respectively) and is sufficient for the implementation of Models 0 and 1.

For the implementation of Model 2, however, it is necessary to estimate G_{ds} and G_{dg} separately. The diffuse irradiance G_{dg} in the collector plane reflected by the ground is estimated from G_h as follows: $G_{dg} = \rho_g\,(1 - \cos\beta)\,G_h/2$. This equation assumes that the ground behaves as a perfect diffuse and isotropic reflector, where ρ_g is the albedo of the ground. Finally, G_{ds} is estimated by difference, $G_{ds} = G_{dt} - G_{dg}$.

With respect to the albedo of the ground, there are two options. The first and more accurate option is to add an albedometer in front of the test platform. This instrument consists of two global pyranometers positioned horizontally, one facing down to measure the solar radiation reflected by the ground. The albedo is then obtained as the ratio of the two measurements. Ideally, these measurements should be synchronized with those of the tested collector to provide albedo values specific to the sky conditions at the time of the test at the specific site. This has the disadvantage of requiring an additional radiometer. The second option is to perform a long asynchronous measurement campaign; one year would be optimal to capture the annual variability of albedo, and use this data to fit an empirical model. This model can then be used to estimate the albedo at the time of the test using the solar irradiance measurements on the horizontal plane mentioned above. This option is less accurate but does not require an additional radiometer at the time of the test.

The second approach was used in this work. In this sense, six empirical albedo models were fitted in Ref. [29] using measurements from the albedometer shown in Figure 1, which is located in front of the collector test platform. For simplicity, the simplest model was used, which results from assuming a constant value for the ground albedo; $\rho_g = 0.2190$, independent of sky conditions. In addition, a sensitivity analysis was conducted to evaluate the impact of varying albedo values on the results. It was found that deviations of $\pm$ 20 % in albedo lead to only $\pm$ 1 % variations in the parameter identification of the collectors, confirming the robustness of the proposed procedure.

Figure 1: Experimental setup to measure the albedo of the ground surrounding the test bench (both instruments on the right; the others are for inclined solar irradiance, not used in this study).

3.2. Experimental data and methodology for assessing diffuse IAM models

In this study, we used test data from two different solar thermal collectors: a Flat Plate Collector, referred to as FPC, and an Evacuated Tube Collector with Heat Pipes, referred as ETC-HP. The FPC served as the reference collector in a previously mentioned inter-laboratory comparison. These collectors and the experimental data set used in this study are identical to those used in Ref. [30]. For this reason, some general details of the tests are given below, but specific details can be found in the aforementioned article.

Testing for the FPC took place from April 30 to May 15, 2021, while the ETC-HP was tested from September 3 to September 30, 2022. All tests followed the ISO 9806:2017 standard. Throughout the experiments, a spatial average wind speed of 3 m/s was maintained using air blowers. In addition, flow rates were set at 2.40 L/min for the FPC and 1.90 L/min for the ETC-HP. Five different measurement sequences were obtained for the FPC and six different sequences for the ETC-HP (due to its complex IAM) using the QDT method. The SST methodology used the same data, but subjected it to different processing procedures to identify the sub-sequences or data points that met the specific requirements of that method.

The methodology used to assess the performance of diffuse IAM models is described as follows. The experimental data previously describe were used to determine the parameters of the thermodynamic model introduced in Eq. (1) for both FPC and ETC-HP collectors, considering the various diffuse IAM models (Model 0, 1 and 2) and associated testing methods (SST and QDT).

The comparison between models was carried out in three steps. First, the parameter values were directly compared (when applicable), with particular attention to the differences arising from the testing methodologies adopted for each diffuse IAM model. Since not all models are directly comparable on a parameter-by-parameter basis, the second step involved calculating the useful energy produced by each collector under the reporting conditions defined in the standard. This approach enables a more comprehensive comparison by capturing the combined effect of all model parameters under varying operating conditions.

Finally, the enhanced parameter conversion from SST to QDT, previously proposed by the authors [7], was evaluated alongside the alternative IAM models to further improve the consistency and reliability of the testing procedures. In particular, this work presents the extension of the enhanced parameter conversion procedure from SST to QDT to Model 2, while the extension for Model 1 was already introduced in previous work.

4. Results

This section presents and discusses the results obtained using the methodology described above. First, Subsection 4.1 shows the fitting results of the different diffuse IAM models along with the corresponding discussion. Next, Subsection 4.2 compares the performance of these models by presenting the useful power

produced by each collector under the reporting conditions defined in the standard. The benefits of the new proposals are highlighted, particularly the improved agreement between the steady-state and quasi-dynamic methods achieved with the new modeling. Finally, Subsection 4.3 presents the results of the enhanced parameter conversion procedure from SST to QDT for all models, which show that combining it with alternative diffuse IAM models further reduces discrepancies between testing methods.

4.1. Models' parameters comparison

Models are implemented and evaluated under the SST and QDT procedures for both collector types. Table 1 and Table 2 show the parameter values of the thermodynamic models from Eq. (1) for FPC and ETC-HP, respectively. Uncertainty is reported only when mandatory according to the standard (i.e., for performance parameters: all parameters except those related to the beam IAM), to simplify the tables. Additionally, uncertainty cannot be reported when a parameter is fixed by the regression algorithm (e.g., when the second-order loss coefficient is set to zero). Moreover, it is not possible to provide uncertainty for the diffuse IAM parameters of the proposed model due to limitations of the method used, as discussed in Subsection 2.4.

The values of the nodes for the angle of incidence modifier are reported every 10 degrees at the bottom part of each table. It is noted that K_{bL} for $\theta_L > 40°$ and K_{bT} for $\theta_T = 80°$ correspond to interpolated data. For all parameters, a t-statistic greater than 3 was obtained, indicating statistical significance, except for the parameter a_2, which therefore had to be kept constant at 0. A data averaging time of 10 minutes was used for the SST method, and a data averaging time of 1 minute was used for the QDT method. In addition, the numerical simulation time step in the dynamic parameter identification algorithm of the QDT was set to 30 seconds, effectively balancing the benefits of the algorithm and its execution time [30].

It is worth noting that, in all cases, the final value of the mean square error (used as the objective function in the parameter identification process) is approximately 2-3 % relative to the mean useful power. This indicates that, for the specific dataset used in this study, the models exhibit a comparable level of accuracy.

For better interpretation of the results, the parameters are divided into two sets. The first set includes the parameters $\eta_{0,b}$, a_1, a_2, a_5, and K_b, while the second set consists of the parameters associated with the diffuse IAM: K_d, K_{ds} and K_{dg}, whenever applicable.

The parameters of the *first set* do not change significantly when considering different models of diffuse IAM within the SST framework. This is due to the fact that in this test method, the determination of the parameters involves a certain degree of independence; the parameters are determined by three independent subtests. On the other hand, in the QDT method, the determination of the parameters is global, i.e., all the parameters are determined simultaneously. Therefore, in this case (QDT), some variation in the parameter values is expected when considering different models of diffuse IAM. However, these variations are minimal,

Table 1: Characteristic parameters of the FPC for each diffuse IAM model and test method. N/A indicates not applicable.

Model	Model 0				Model 1				Model 2			
Test	SST		QDT		SST		QDT		SST		QDT	
method	Value	Uncer.	Value	Uncer.	Value	Uncer.	Value	Uncer.	Value	Uncer.	Value	Uncer.
$\eta_{0,b}$	0.726	N/A	0.720	±0.001	0.726	N/A	0.722	±0.001	0.727	N/A	0.721	±0.001
a_1	4.499	±0.019	4.331	±0.020	4.499	±0.019	4.342	±0.021	4.499	±0.019	4.340	±0.020
a_2	0	N/A	0.001	±0.0003	0	N/A	0.001	±0.0003	0	N/A	0.001	±0.0003
$a_5 \times 1000$	11.0	±0.6	12.7	±0.1	11.0	±0.6	12.5	±0.1	11.0	±0.6	12.6	±0.1
K_d	0.905	N/A	0.941	±0.004	0.905	N/A	0.895	N/A	–	–	–	–
K_{ds}	–	–	–	–	–	–	–	–	0.933	N/A	0.913	N/A
K_{dg}	–	–	–	–	–	–	–	–	0.744	N/A	0.717	N/A
θ	K_b		K_b		K_b		K_b		K_b		K_b	
0	1.00		1.00		1.00		1.00		1.00		1.00	
10	1.00		0.99		1.00		1.00		1.00		1.00	
20	1.00		0.99		1.00		0.99		1.00		0.99	
30	1.00		0.98		1.00		0.99		1.00		0.99	
40	1.00		0.98		1.00		0.98		1.00		0.98	
50	0.97		0.94		0.97		0.95		0.97		0.95	
60	0.90		0.87		0.88		0.88		0.88		0.88	
70	0.72		0.68		0.68		0.73		0.68		0.71	
80	0.36		0.34		0.34		0.37		0.34		0.35	
90	0		0		0		0		0		0	

in the order of 1 % in most cases. When comparing the test methods between themselves, it can be seen that for most parameters the differences are small, usually below 10 %, except for a_5 and $K_b(\theta \geq 60°)$, where the differences are between about 17 % and 50 %, being larger in the case of ETC-HP. These differences are in line with previous work [10].

Regarding the *second set*, the parameters of Models 0 and 1 are directly comparable, since both consider the diffuse component globally, assuming a constant value for the parameter K_d. Therefore, we will start with the analysis of these models. In the case of the SST method, the parameter K_d is the same in both models, as expected since it is estimated in the same way (see Subsection 2.3). In the case of the QDT method, it is observed that the value of K_d for Model 1 is quite close to that of the SST, while in the case of Model 0 it is not. Specifically, this parameter is overestimated in the QDT by 4 % and 20 % for the FPC and ETC-HP collectors, respectively, a result that is consistent with previous research [7, 9, 10]. This can be explained as follows. Although Models 0 and 1 consider K_d as a constant, the way in which this constant is determined is different in each case. As explained in Subsection 2.3, in the case of Model 0 for QDT,

Table 2: Characteristic parameters of the ETC-HP for each diffuse IAM model and test method. N/A indicates not applicable.

Collector	Model 0				Model 1				Model 2			
Test	SST		QDT		SST		QDT		SST		QDT	
method	Value	Uncer.	Value	Uncer.	Value	Uncer.	Value	Uncer.	Value	Uncer.	Value	Uncer.
$\eta_{0,b}$	0.371	N/A	0.365	±0.0003	0.371	N/A	0.373	±0.0003	0.372	N/A	0.371	±0.0003
a_1	1.682	±0.060	1.678	±0.005	1.682	±0.060	1.703	±0.006	1.68	±0.060	1.693	±0.006
a_2	0	N/A	0	N/A	0	N/A	0	0	0	N/A	0	N/A
$a_5 \times 1000$	207.6	±1.0	167.8	±0.9	207.6	±1.0	172.0	±1.1	207.6	±1.0	170.2	±0.9
K_d	1.007	N/A	1.235	±0.004	1.007	N/A	1.084	N/A	–	–	–	–
K_{ds}	–	–	–	–	–	–	–	–	1.055	N/A	1.131	N/A
K_{dg}	–	–	–	–	–	–	–	–	0.671	N/A	0.775	N/A
$\theta_L \backslash \theta_T$	K_{bL}	K_{bT}	K_{bL}	K_{bT}	K_{bL}	K_{bT}	K_{bL}	K_{bT}	K_{bL}	K_{bT}	K_{bL}	K_{bT}
0	1.00	1.00	1.00	1.00	1.00	1.00	1.00	1.00	1.00	1.00	1.00	1.00
10	0.99	1.01	0.98	1.00	0.99	1.01	0.99	0.99	0.99	1.01	0.99	0.99
20	0.99	1.07	1.00	1.09	0.99	1.07	1.00	1.09	0.99	1.07	1.00	1.09
30	1.00	1.15	1.00	1.18	1.00	1.15	1.00	1.19	1.00	1.15	1.00	1.19
40	0.97	1.29	1.00	1.36	0.97	1.29	1.00	1.36	0.97	1.29	1.00	1.36
50	0.77	1.40	0.80	1.57	0.77	1.40	0.80	1.57	0.77	1.40	0.80	1.57
60	0.58	1.44	0.60	1.56	0.58	1.44	0.60	1.57	0.58	1.44	0.60	1.57
70	0.39	1.18	0.40	1.74	0.39	1.18	0.40	1.77	0.39	1.18	0.40	1.76
80	0.19	0.59	0.2	0.87	0.19	0.59	0.20	0.88	0.19	0.59	0.2	0.88
90	0	0	0	0	0	0	0	0	0	0	0	0

this parameter is fitted to the experimental data, including possible biases in the distribution of the samples with respect to the sky conditions. In the case of Model 1, the K_d parameter is determined by integrating and weighting the K_b function over the solid angle seen by the collector, in the same way as in the SST method; hence, the differences are smaller. In summary, Model 1 provides greater agreement between the SST and QDT test methods.

For Model 2, the parameters of this model are determined separately, as this model treats diffuse solar irradiance differently from Models 0 and 1. This model distinguishes between diffuse solar irradiance coming from the sky and that reflected from the ground, with a parameter for each component, K_{ds} and K_{dg}. The values of the parameters depend on the horizontal tilt of the collector; for a simple comparison, a horizontal tilt of 45° was used. The agreement between the SST and QDT test methods is better than for Model 0, but slightly worse than for Model 1. The main discrepancy is observed in the parameter K_{dg}, and the determination of this parameter is strongly influenced by the nodal values of the K_{bL} function at high angles of incidence, which have greater uncertainty.

As the parameters of Model 2 cannot be directly compared with those of Models 0 and 1, the next section provides a comparative analysis in terms of the useful power produced by the collectors. This will provide a better understanding of the differences between the models.

4.2. Useful power under standard reporting conditions

To complement the results and discussion presented in the previous section, the useful power produced by each collector was calculated for different temperature differences and sky conditions using Eq. (1) for Models 0 and 1, and Eq. (9) for Model 2. In all cases, normal incidence and steady-state conditions were assumed, as specified in the ISO 9806:2017 standard. For the temperature difference, four cases were considered: 0, 20, 40 and 60 K. For the sky conditions, the Standard Reporting Conditions (SRC) specified in the ISO 9806:2017 standard were used, as shown in Table 3. In addition, the evaluation of Model 2 requires the specific values of G_{ds} and G_{dg}. The diffuse solar irradiance reflected by the ground G_{dg} was estimated using Eq. (11), a relationship derived using the isotropic transposition model [15], assuming normal incidence and $G_{dh}/G_h \approx G_{dt}/G_t$.

$$G_{dg} = G_{dt}\,\frac{\rho\,(1-\cos\beta)}{(G_{dt}/G_t)(1+\cos\beta)+\rho\,(1-\cos\beta)}. \tag{11}$$

Then the diffuse solar irradiance from the sky was estimated by the difference, i.e.: $G_{ds} = G_{dt} - G_{dg}$. These expressions were evaluated assuming an albedo of 0.2 and a horizontal tilt of 45°, and their results are shown in the last two columns of Table 3. These values (albedo and tilt) are commonly used in the field of solar thermal testing [15].

Table 3: Standard Reporting Conditions (SRC).

Solar irradiance	G_{bt} (W/m^2)	G_{dt} (W/m^2)	G_{ds} (W/m^2)	G_{dg} (W/m^2)
Blue Sky	850	150	121	29
Hazy Sky	440	260	239	21
Gray Sky	0	400	287	13

The useful power estimates for the different cases are shown in Figure 2 and Figure 3 for FPC and ETC-HP respectively. For a better understanding of these figures, note that each column corresponds to a different diffuse IAM model; Model 0, 1, and 2 from left to right, and each row corresponds to a different sky condition: clear, hazy, and gray sky, from top to bottom. In general, no significant differences are observed for clear sky conditions. However, for hazy and gray sky conditions, the differences between the test methods and the models become evident and tend to increase with the diffuse fraction. In terms of temperature differences, the discrepancy between test methods and models becomes more pronounced at

higher values. These observations are more pronounced for the ETC-HP collector (Figure 3) than for the FPC collector (Figure 2).

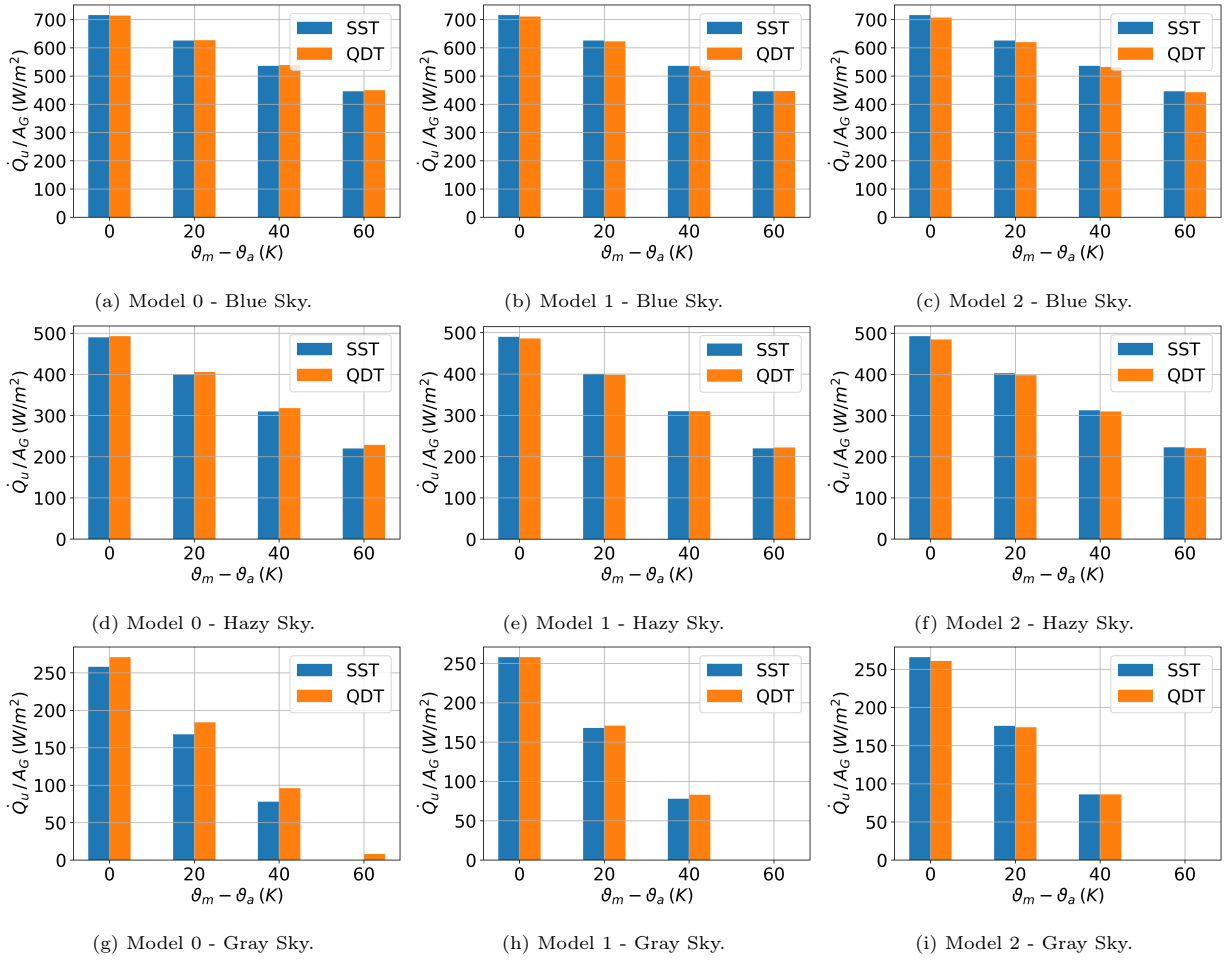

(a) Model 0 - Blue Sky. (b) Model 1 - Blue Sky. (c) Model 2 - Blue Sky.

(d) Model 0 - Hazy Sky. (e) Model 1 - Hazy Sky. (f) Model 2 - Hazy Sky.

(g) Model 0 - Gray Sky. (h) Model 1 - Gray Sky. (i) Model 2 - Gray Sky.

Figure 2: Useful power per gross area unit produced by FPC collector under standard reporting conditions, for each test method and diffuse IAM model.

The following procedure was used to analyze the consistency of the test methods. First, the difference between SST and QDT useful power estimates was calculated for the different sky conditions and temperature differences, and then all the differences were averaged for each diffuse IAM model. Finally, the models were ranked in decreasing order, from the least consistent to the most consistent, i.e. from the largest difference to the smallest average difference. This procedure was done separately for each collector.

For FPC, the models are ordered as follows: Model 0, 2, and 1, with average differences of 3.3 %, 1.6 %, and 0.6 %, respectively. In this case, the difference between the models is small, consistent with Figure 2. For ETC, the models are ordered as follows: Model 0, 1, and 2, with average differences of 16 %, 6.7 %, and 5.2 %, respectively. In this case, the differences are significant, especially for Model 0. Although Model 2 is

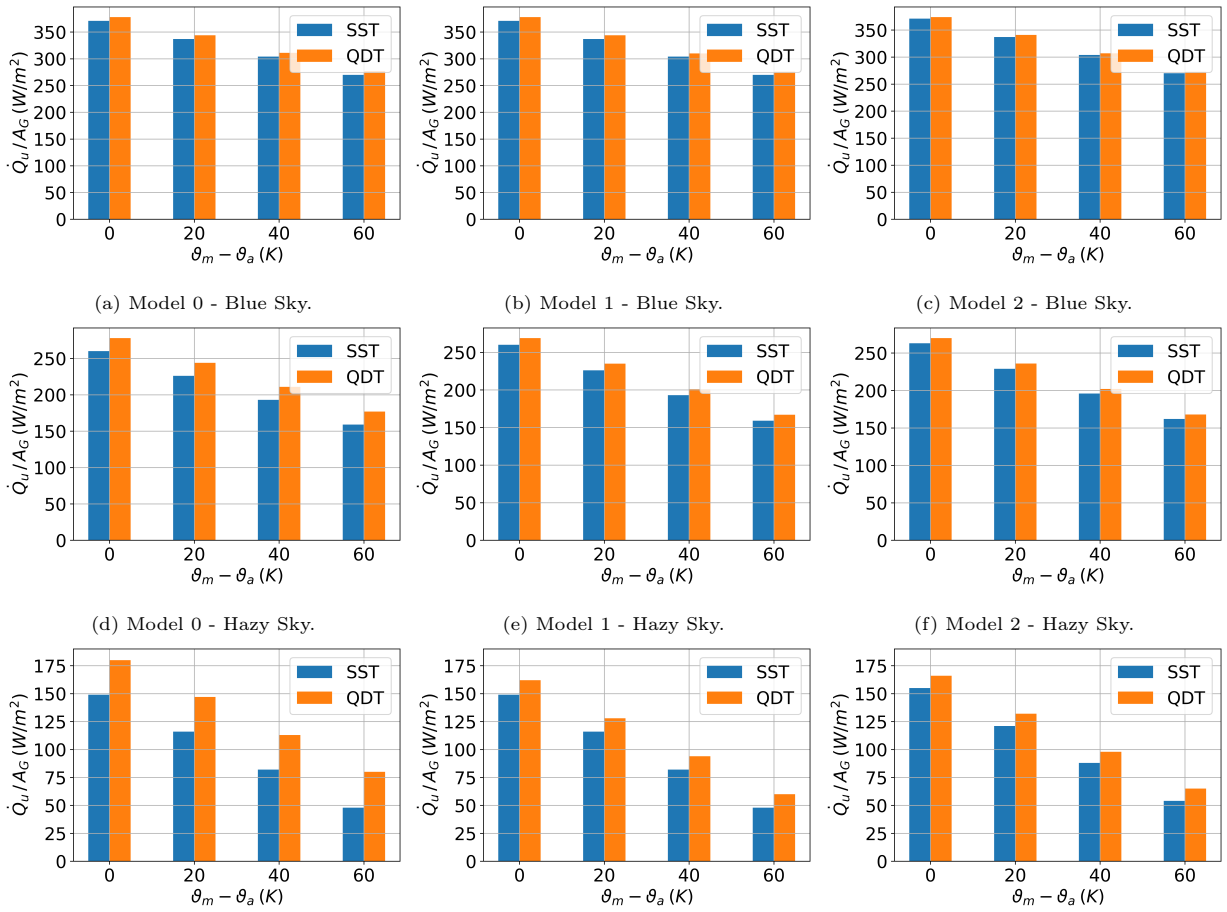

(a) Model 0 - Blue Sky. (b) Model 1 - Blue Sky. (c) Model 2 - Blue Sky.

(d) Model 0 - Hazy Sky. (e) Model 1 - Hazy Sky. (f) Model 2 - Hazy Sky.

(g) Model 0 - Gray Sky. (h) Model 1 - Gray Sky. (i) Model 2 - Gray Sky.

Figure 3: Useful power per gross area unit produced by ETC-HP collector under standard reporting conditions, for each test method and diffuse IAM model.

better than Model 1, the difference between these models is small, as shown in Figure 3. It should also be noted that the percentages above are averages and therefore indicative. They do not reflect the asymmetry of the differences in sky conditions and temperature differences (see Figures 2 and 3). In general, as mentioned above, the differences are much larger for hazy sky conditions and high temperature conditions.

In summary, Models 1 and 2 significantly improve the consistency between test methods compared to Model 0. However, the differences between Models 1 and 2 are small, so considering the additional cost of the additional albedo measurement, we consider Model 1 to be the ideal choice for testing the solar collector technology considered in this work. However, for other technologies, for example those that are particularly sensitive to diffuse solar irradiance [16], Model 2 may be the better choice for testing due to its superior performance, allowing for a better evaluation of design improvements and/or the use of alternative materials.

Furthermore, since the values of K_b obtained during the tests do not change when considering different

models of diffuse IAM (as demonstrated in the previous section), Models 1 and 2 can be used in a complementary way, as described below. Once the parameters have been determined with Model 1 in the context of the normalized tests, it would be possible to use Model 2 to carry out a long-term performance simulation, reconstructing the parameters of this model, i.e. calculating K_{ds} and k_{dg} from Eqs. (6) and (7) respectively, using the previously determined value of K_b with Model 1.

4.3. Enhanced parameter conversion from SST to QDT

In previous work [7], an enhanced parameter conversion procedure from SST to QDT was proposed, in which the procedure was applied to two ETC-HP collectors. It was shown that this procedure is better than that of the standard, since it produces converted IAM values closer to the QDT method. The above work covers Models 0 and 1, as the models are the same for the SST method. This subsection demonstrates the extension of this procedure for Model 2 and both collector types: FPC and ETC-HP.

The standard conversion procedure was described in Section 2. The extended procedure for Models 0 and 1, although detailed in [7], is briefly described below. First, we assume initial values for $\eta_{0,b}$ and K_d (which could be those of the standard conversion). Next, we compute K_b using Eq. (12) (instead of assuming $K_{hem} = K_b$), and then we recompute the parameters $\eta_{0,b}$ and K_d as in the standard case; Eqs. (4) and (5). The iterative process continues until the difference between the input and output parameters is less than a specified tolerance. For Model 2, the process is similar, but it uses Eq. (13) instead of Eq. (12), and Eqs. (6), (7) and (10) instead of Eqs. (4) and (5).

$$K_b = \frac{(\eta_{0,hem}/\eta_{0,b})\ K_{hem}\ G_t - K_d\ G_{dt}}{G_{bt}}. \tag{12}$$

$$K_b = \frac{(\eta_{0,hem}/\eta_{0,b})\ K_{hem} - K_{ds}\ G_{ds} - K_{dg}\ G_{dg}}{G_{bt}}. \tag{13}$$

The results of the standard and improved parameter conversion are shown in Table 4 for both collectors.

In the case of the FPC collector, although the enhanced procedure gives results closer to the QDT, the differences with the standard procedure are minimal. In the case of the ETC-HP collector, the results are much more significant: the improved procedure gives better IAM values (direct and diffuse), i.e. closer to those obtained by the QDT method.

In this context, the useful power values presented in the previous subsection were recalculated for the SST method using the diffuse IAM obtained through the enhanced procedure. For the FPC collector, no significant differences were observed. In contrast, for the ETC-HP collec, the average difference between SST and QDT estimates decreased by approximately 2 to 3 percentage points when considering all sky conditions, and by 5 to 10 percentage points under gray sky conditions. These results confirm that the enhanced procedure effectively reduces discrepancies between SST and QDT, particularly under hazy or overcast conditions.

Table 4: Comparison between standard and enhanced parameter conversion from SST to QDT for both collector and the different diffuse IAM models.

Collector	FPC				ETC-HP							
Model	Model 0 and 1		Model 2		Model 0 and 1				Model 2			
Conversion	Standard	Enhanced	Standard	Enhanced	Standard		Enhanced		Standard		Enhanced	
$\eta_{0,b}$	0.726	0.727	0.727	0.728	0.371		0.369		0.375		0.370	
K_d	0.905	0.896	N/A	N/A	1.007		1.039		N/A		N/A	
K_{ds}	N/A	N/A	0.933	0.925	N/A		N/A		1.055		1.095	
K_{dg}	N/A	N/A	0.744	0.717	N/A		N/A		0.671		0.702	
θ	K_b	K_b	K_b	K_b	K_{bL}	K_{bT}	K_{bL}	K_{bT}	K_{bL}	K_{bT}	K_{bL}	K_{bT}
0	1.00	1.00	1.00	1.00	1.00	1.00	1.00	1.00	1.00	1.00	1.00	1.00
10	1.00	1.00	1.00	1.00	0.99	1.01	1.00	1.01	0.99	1.01	1.00	1.01
20	1.00	1.00	1.00	1.00	0.99	1.07	1.00	1.08	0.99	1.07	1.00	1.08
30	1.00	1.00	1.00	1.00	1.00	1.15	1.00	1.18	1.00	1.15	1.00	1.18
40	1.00	1.00	1.00	1.00	0.97	1.29	0.97	1.34	0.97	1.29	0.97	1.34
50	0.97	0.97	0.97	0.96	0.77	1.40	0.78	1.48	0.77	1.40	0.78	1.48
60	0.90	0.88	0.90	0.87	0.58	1.44	0.58	1.54	0.58	1.44	0.58	1.54
70	0.72	0.68	0.72	0.67	0.39	1.18	0.39	1.27	0.39	1.18	0.39	1.27
80	0.36	0.34	0.36	0.34	0.19	0.59	0.19	0.64	0.19	0.59	0.19	0.63
90	0	0	0	0	0	0	0	0	0	0	0	0

As for the comparison between models, no significant differences were found between Models 1 and 2. This suggests that the enhanced procedure benefits both models similarly, and the conclusions drawn in the previous section regarding their performance remain valid.

5. Conclusions

In this work, two different diffuse IAM models for solar thermal collectors have been integrated into the standard test method of ISO 9806:2017; Model 1 and Model 2. The first model treats the diffuse in a global manner, and the second model distinguishes between the direction, that from the sky and that reflected from the ground, requiring an additional measurement for the latter component. The performance of these models has been evaluated and compared with the standard model, which serves as a baseline, using test data from two different solar collectors: a Flat Plate Collector (FPC) and an Evacuated Tube Collector with Heat Pipe (ETC-HP). The evaluation was performed using both ISO 9806:2017 test methods: steady-state (SST) and quasi-dynamic (QDT).

First, the parameter values of each collector and diffuse IAM model were identified. The results showed

that all the parameter values, except those related to the diffuse IAM, are very similar and independent of the diffuse IAM chosen. On the other hand, in the case of the parameters related to the diffuse IAM, Models 1 and 2 show a much better test method coherence, i.e. the parameter values obtained by the SST and QDT methods are closer.

However, the parameters of Models 1 and 2 cannot be directly compared due to the different way in which the diffuse solar radiation is treated. In this sense, for a better comparison of these models and using the previously determined parameter values, the useful power produced by the collectors was calculated and compared. For the temperature difference, four cases were considered: 0, 20, 40 and 60 K and for the sky conditions, the Standard Reporting Conditions (SRC) specified in the ISO 9806:2017 standard were used. Overall, no significant differences are found under clear sky conditions. However, under hazy and overcast conditions, differences between the test methods and the models become significant. Regarding temperature differences, the differences between test methods and models become more pronounced at higher values. These trends are particularly pronounced for ETC-HP. It is observed that Models 1 and 2 improve the consistency between test methods.

Nevertheless, the differences between Models 1 and 2 are small, so the loss of precision associated with the global modeling of diffuse irradiance does not compensate for the additional measurement for Model 2. Therefore, we consider Model 1 to be the best choice for evaluating the solar collector technology considered in this work. However, for technologies more sensitive to diffuse solar irradiance, Model 2 may be more suitable. Furthermore, as the K_b values obtained during testing remain unchanged across models, they can be used complementarily: first, Model 1 for standardized testing, and then Model 2 for long-term simulations, reconstructing its parameters from those obtained with Model 1.

Furthermore, the improved parameter conversion from SST to QDT proposed by Rodríguez-Muñoz et al. has been extended and evaluated in combination with the diffuse IAM models considered in this work. This procedure improves even more the consistency between the test methods, especially in the case of ETC-HP, providing IAM values (direct and diffuse) that are closer and reducing the differences in the estimated useful power for the collectors. In the case of FPC, although the enhanced procedure gave better results, the difference with the standard procedure was small.

It is important to mention that all tests were carried out with a low albedo soil, as specified by the standard. It is to be expected that the differences between Models 1 and 2 will be more considerable when working with higher albedo soils, e.g. in the framework of in-situ tests. The analysis of more complex terrains represents future work.

Acknowledgments

The authors extend their gratitude to the Ministerio de Industria, Energía y Minería (MIEM, Uruguay), particularly the Dirección Nacional de Energía (DNE), the Fideicomiso Uruguayo de Ahorro y Eficiencia Energética (Fudaee, Uruguay), and the Corporación Nacional para el Desarrollo (CND, Uruguay) for their financial and logistical support in developing the BECS facility and fostering this project with local expertise. Special thanks also go to the PTB of Germany for promoting and funding the interlaboratory test on solar collector efficiency, which provided valuable technical assurance of our local testing capabilities. The authors acknowledge financial support from the CSIC Research Group Program, Universidad de la República, Uruguay.

Appendix A. Data and software availability

To facilitate the application of the QDT method, a MATLAB program with a nonlinear regression algorithm is available for download: https://bit.ly/STCT-Program-V3. This program is designed for general use with low-temperature solar collectors that have covers, supporting both uniaxial and biaxial IAM. It builds on the previous versions of the software provided in [7, 30], making this the third version, which retains the options from the earlier versions. In this version, three models for diffuse IAM (Model 0, 1, and 2, as discussed in this study) are included.

The program calculates and reports the characteristic parameter values along with their uncertainties and t-statistics (the ratio of the parameter value to its uncertainty). For parameter a_2, users can set custom upper and lower limits, allowing it to be fixed at zero if the t-statistic is below 3 (both limits must be set to zero in this case). The software does not verify the quality of the experimental data set or ensure compliance with the ISO 9806:2017 standard, which must be checked beforehand. However, it provides graphs to evaluate data variability. The software also includes the two experimental data sets used in this study.

References

[1] G. Abal, D. Aicardi, R. Alonso-Suárez, A. Laguarda, Performance of empirical models for diffuse fraction in uruguay, Solar Energy 141 (2017) 166 – 181. doi:https://doi.org/10.1016/j.solener.2016.11.030.

[2] ISO-9806, Solar energy – solar thermal collectors – test methods, Standard, International Organization of Standarization, Switzerland (2017).

[3] ASHRAE-93, Methods of testing to determine the thermal performance of solar collectorss, Standard, American Society of Heating, Refrigerating and Air-Conditioning Engineers, USA (2014).

[4] D. Rojas, J. Beermann, S. Klein, D. Reindl, Thermal performance testing of flat-plate collectors, Solar Energy 82 (8) (2008) 746 – 757. doi:https://doi.org/10.1016/j.solener.2008.02.001.

[5] P. Horta, M. J. Carvalho, M. C. Pereira, W. Carbajal, Long-term performance calculations based on steady-state efficiency test results: Analysis of optical effects affecting beam, diffuse and reflected radiation, Solar Energy 82 (11) (2008) 1076–1082. doi:https://doi.org/10.1016/j.solener.2008.01.004.

[6] J. M. Rodríguez-Muñoz, I. Bove, R. Alonso-Suárez, Novel incident angle modifier model for quasi-dynamic testing of flat plate solar thermal collectors, Solar Energy 224 (2021) 112–124. doi:https://doi.org/10.1016/j.solener.2021.05.026.

[7] J. M. Rodríguez-Muñoz, I. Bove, R. Alonso-Suárez, Improving the experimental estimation of the incident angle modifier of evacuated tube solar collectors with heat pipes, Renewable Energy 235 (2024) 121240. doi:https://doi.org/10.1016/j.renene.2024.121240.

[8] P. Kovács, U. Pettersson, M. Persson, B. Perers, S. Fischer, Improving the accuracy in performance prediction for new collector designs, in: Proceedings of Solar World Congress, 2011.

[9] E. Zambolin, D. Del Col, An improved procedure for the experimental characterization of optical efficiency in evacuated tube solar collectors, Renewable Energy 43 (2012) 37 – 46. doi:https://doi.org/10.1016/j.renene.2011.11.011.

[10] T. Osório, M. J. Carvalho, Testing of solar thermal collectors under transient conditions, Solar Energy 104 (2014) 71 – 81, solar heating and cooling. doi:https://doi.org/10.1016/j.solener.2014.01.048.

[11] S. Fischer, W. Heidemann, H. Müller-Steinhagen, B. Perers, P. Bergquist, B. Hellström, Collector test method under quasi-dynamic conditions according to the european standard en 12975-2, Solar Energy 76 (1) (2004) 117 – 123. doi:https://doi.org/10.1016/j.solener.2003.07.021.

[12] M. Bosanac, A. Brunotte, W. Spirkl, R. Sizmann, The use of parameter identification for flat-plate collector testing under non-stationary conditions, Renewable Energy 4 (2) (1994) 217–222.

[13] M. J. Carvalho, P. Horta, J. F. Mendes, M. C. Pereira, W. M. Carbajal, Incidence angle modifiers: A general approach for energy calculations, in: D. Y. Goswami, Y. Zhao (Eds.), Proceedings of ISES World Congress 2007 (Vol. I – Vol. V), Springer Berlin Heidelberg, Berlin, Heidelberg, 2009, pp. 608–612.

[14] M. Brandemuehl, W. Beckman, Transmission of diffuse radiation through cpc and flat plate collector glazings, Solar Energy 24 (5) (1980) 511–513. doi:https://doi.org/10.1016/0038-092X(80)90320-5.

[15] J. Duffie, W. Beckman, Solar Engineering of Thermal Processes, 3rd Edition, Wiley and Sons, Inc., Hoboken, New Jersey, 2006.

[16] S. Hess, V. I. Hanby, Collector simulation model with dynamic incidence angle modifier for anisotropic diffuse irradiance, Energy Procedia 48 (2014) 87–96, proceedings of the 2nd International Conference on Solar Heating and Cooling for Buildings and Industry (SHC 2013). doi:https://doi.org/10.1016/j.egypro.2014.02.011.

[17] A. P. Brunger, F. C. Hooper, Anisotropic sky radiance model based on narrow field of view measurements of shortwave radiance, Solar Energy 51 (1) (1993) 53 – 64. doi:https://doi.org/10.1016/0038-092X(93)90042-M.

[18] J. M. Rodríguez-Muñoz, G. Vitale, I. Bove, G. Abal, Directional anisotropy of diffuse solar irradiance: impact assessment on the solar transmittance of common glazings, Building Simulation Conference Proceedings 18 (2023) 3832–3839.

[19] B. Perers, An improved dynamic solar collector test method for determination of non-linear optical and thermal characteristics with multiple regression, Solar Energy 59 (4) (1997) 163 – 178. doi:https://doi.org/10.1016/S0038-092X(97)00147-3.

[20] A. Hofer, D. Büchner, K. Kramer, S. Fahr, A. Heimsath, W. Platzer, S. Scholl, Comparison of two different (quasi-) dynamic testing methods for the performance evaluation of a linear fresnel process heat collector, Energy Procedia 69 (2015) 84–95, international Conference on Concentrating Solar Power and Chemical Energy Systems, SolarPACES 2014. doi:https://doi.org/10.1016/j.egypro.2015.03.011.

[21] S. Fahr, U. Gumbel, A. Zirkel-Hofer, K. Kramer, In situ characterization of thermal collectors in field installations, in: Proceedings of EuroSun, 2018. doi:0.18086/eurosun2018.12.01.

[22] A. Zirkel-Hofer, S. Perry, K. Kramer, A. Heimsath, S. Scholl, W. Platzer, Confidence interval computation method for

dynamic performance evaluations of solar thermal collectors, Solar Energy 162 (2018) 585–596. doi:https://doi.org/10.1016/j.solener.2018.01.041.
URL https://www.sciencedirect.com/science/article/pii/S0038092X18300628

[23] J. C. Rodrigues, J. Facão, M. J. Carvalho, Parameter identification and uncertainty evaluation in quasi-dynamic test of solar thermal collectors with monte carlo method, Renewable Energy 236 (2024) 121403. doi:https://doi.org/10.1016/j.renene.2024.121403.
URL https://www.sciencedirect.com/science/article/pii/S096014812401471X

[24] S. Fischer, Quality infrastructure for energy efficiency and renewable energy in latin america and the caribbean, report # 95309, Report, Intituto Metrológico Aleman - PTB (2020).

[25] ISO-9060, Solar energy — specification and classification of instruments for measuring hemispherical solar and direct solar radiation, Standard, International Organization of Standarization, Switzerland (2018).

[26] ISO-9847, Solar energy – calibration of field pyranometers by comparison to a reference pyranometer, Standard, International Organization of Standarization, Switzerland (1992).

[27] J. M. Rodríguez-Muñoz, A. Monetta, R. Alonso-Suárez, I. Bove, G. Abal, Correction methods for shadow-band diffuse irradiance measurements: assessing the impact of local adaptation, Renewable Energy 178 (2021) 830–844. doi:https://doi.org/10.1016/j.renene.2021.06.102.

[28] A. J. Drummond, On the measurement of sky radiation, Archiv für Meteorologie, Geophysik und Bioklimatologie, Serie B 7 (1956) 413 – 436. doi:https://doi.org/10.1007/BF02242969.

[29] J. M. Rodríguez-Muñoz, R. Alonso-Suárez, I. Bove, G. Abal, Evaluación de seis modelos empíricos para estimar albedo del suelo en la pampa húmeda, Avances en Energías Renovables y Medio Ambiente-AVERMA 26 (2022) 357–368.

[30] J. M. Rodríguez-Muñoz, I. Bove, R. Alonso-Suárez, P. Galione, On the choice of the parameter identification procedure in quasi-dynamic testing of low-temperature solar collectors, Renewable Energy 247 (2025) 122931. doi:https://doi.org/10.1016/j.renene.2025.122931.